

A phantom force induced by the tunneling current, characterized on Si(111)

A.J. Weymouth, T. Wutscher, J. Welker, T. Hofmann, and F.J. Giessibl

Institute of Experimental and Applied Physics, University of Regensburg, D-93053 Regensburg, Germany.

(Dated: July 28, 2021)

Simultaneous measurements of tunneling currents and atomic forces on surfaces and adsorbates provide new insights into the electronic and structural properties of matter on the atomic scale. We report on experimental observations and calculations of a strong impact the tunneling current can have on the measured force, which arises when the resistivity of the sample cannot be neglected. We present a study on Si(111)-7×7 with various doping levels, but this effect is expected to occur on other low-conductance samples like adsorbed molecules, and is likely to strongly affect Kelvin probe measurements on the atomic scale.

Scanning tunneling microscopy (STM) sparked enthusiasm in scanning probe microscopy with images of the adatoms of Si(111)-7×7 [1]. The atomic force microscope (AFM) removed the requirement for a conducting substrate [2] but brought more than just the possibility to measure on insulators [3]: Subatomic [4] and submolecular [5] imaging have also been demonstrated. These successes have brought strong interest in combined STM and AFM (e.g. [6]), however the independence of force and current measurements remains an open issue [7–11].

Frequency-modulation AFM (FM-AFM) is a technique in which the interaction between tip and sample is measured by the frequency shift, Δf , of an oscillating tip from its eigenfrequency, f_0 [12]. Δf can be formulated as a measure of the force gradient, $k_{ts} = -\frac{dF}{dz}$, where z is the distance from the surface. Δf is also a function of the spring constant of the oscillator, k , the amplitude of oscillation, A , and z , and can be approximated at small amplitudes by $\Delta f \approx (f_0/2k) k_{ts}$ [13]. In short, a decrease in Δf indicates that the force between the tip and sample is becoming more attractive.

In contrast to the tunneling current, I , measured with STM, Δf is not monotonic as a function of z . The local tip-sample interaction is usually well-represented by a Morse potential from which the force and the force gradient can be derived, as shown in Fig. 1(a). In region I, k_{ts} decreases as z decreases. Long-range forces (e.g. van der Waals) cause attractive interaction between tip and sample. It is in this region STM is usually conducted on Si(111)-7×7, at setpoints under 10 nA at 1 V, corresponding to tip-sample distances greater than 5 Å [14]. In region II, k_{ts} increases as z decreases. The waveform overlap between tip and sample causes measurable energy increase due to Pauli repulsion, which states electrons may not occupy the same quantum state [15].

In this Letter, we report upon the effect of bias voltage on FM-AFM of Si(111)-7×7. At tip-sample distances corresponding to normal STM setpoints, one expects a decrease in frequency shift as the tip moves laterally without feedback over an adatom, due to the increase in attractive force [16]. However, with the application of a moderate bias voltage (>1.0 V), one is able to observe a frequency shift increase as the tip moves over an adatom.

Moreover, FM-AFM images taken with this applied bias voltage can show atomic contrast at tip-sample distances 300 pm further from the surface than is required to image with no applied bias. We propose a model incorporating sample resistance where the observed frequency shift is caused by a decrease in the electrostatic attraction between tip and sample.

Experiments were performed with a qPlus sensor with $k = 1800 \text{ N m}^{-1}$. Data were collected in constant height mode with both a home-built microscope operating at room temperature in UHV and, where explicitly stated, at 4.2 K with an Omicron LT-SPM. Two types of Si(111) samples were used: a high-doped sample corresponding to a resistivity $\rho = 0.010 - 0.012 \Omega \text{ cm}$ at 300 K and a low-doped sample with $\rho = 6 - 9 \Omega \text{ cm}$ at 300 K. Si(111)-7×7 was prepared with several flash and anneal cycles.

Figure 1(b) to (e) show simultaneously acquired I and Δf data of the low-doped Si(111) sample. In (b) and (c), the tip bias was $V_{\text{tip}} = -1.5 \text{ V}$. STM data show the clear structure of the 7×7 reconstruction, with all adatoms in the unit cell having approximately the same intensity. The Δf data show an increase in frequency shift above adatoms. In (d) and (e), the tip bias was $V_{\text{tip}} = +1.5 \text{ V}$. The STM data show different features now in the outlined unit cell: over adatoms in the faulted half (the lower six adatoms), we record greater absolute current than those in the unfaulted half, as expected [17]. The Δf data, however, also have stronger contrast above the faulted half unit cell. In a simple picture of AFM in which the total electron density is measured [18], one would not expect this Δf contrast to depend upon bias voltage. Also, while one might initially propose that this increase in Δf over adatoms indicates that we are in region II of the Morse potential, we show later (with respect to the data in Fig. 3) that this is not the case.

The relation between Δf and I channels can be further characterized. For each pixel in image Fig. 1(b) to (e), force and current data have been acquired. Before a pixel-by-pixel comparison of I and Δf can be made, however, the low bandwidth of the PLL must be taken into account. At scan speeds even as low as 20 nm s^{-1} , it can cause a noticeable lateral displacement between Δf and I data. Consider a scan line 10 nm long with 256

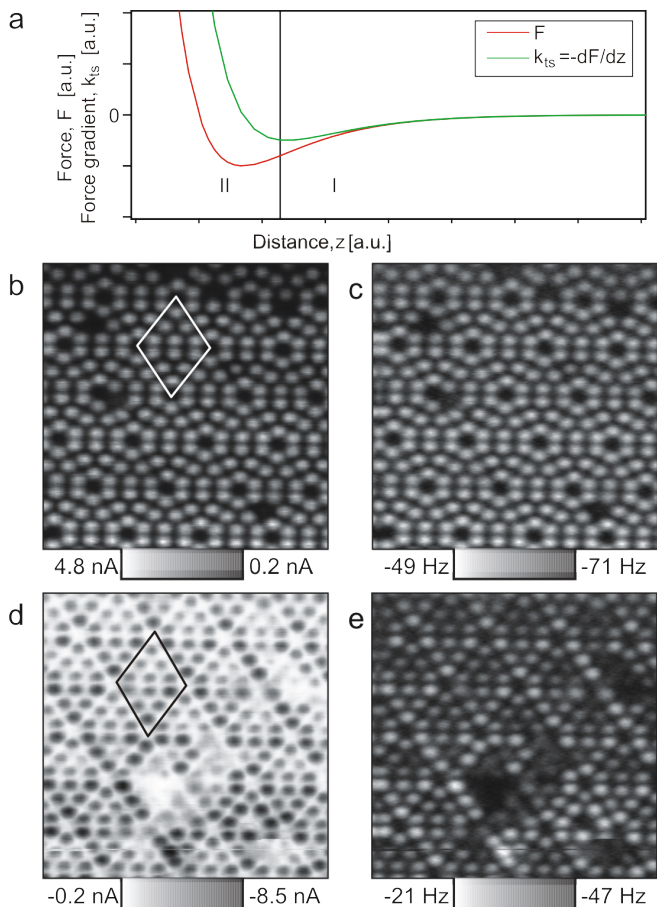


FIG. 1. a) From a Morse potential, the force and force gradient can be calculated. At $V_{\text{tip}} = -1.5$ V, simultaneous b) current and c) force data are collected without I or Δf feedback. Similar data are collected at $V_{\text{tip}} = +1.5$ V; the d) current data appears to be inverted because in opposite bias voltages, current flow is reversed, however e) Δf again increases above adatoms. Data were collected at $A = 400$ pm, $f_0 = 25908$ Hz. In STM data, a unit cell of 7×7 is highlighted; images are $10 \text{ nm} \times 10 \text{ nm}$.

pixels. The bandwidth of our PLL is 120 Hz. Assuming the I data to be instantaneous, the Δf data will be offset by $(256 \text{ pixels}/10 \text{ nm}) \cdot 20 \text{ nm s}^{-1} / 120 \text{ Hz} \approx 4$ pixels. Independently, a cross correlation of Fig. 1(b) and (c) show a 4 pixel offset.

Each measurement of I thus has an associated Δf measurement, and these are plotted (for the Δf and I data shown in Fig. 1 (b) and (c)) in Fig. 2(a). The fact that there is some correspondance does not come as a surprise, as regularly force and current images of the same surface appear similar. What is surprising is that the data are quite linear and yield an increasing frequency shift over the entire current range.

The slope of the linear fit to the data in Fig. 2(a) is a measure of the Δf response as a function of I . This analysis was repeated with images at various bi-

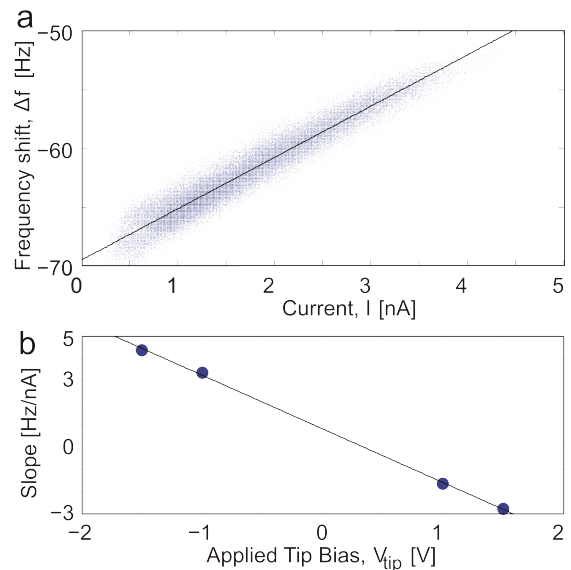


FIG. 2. a) From Fig 1(b) and (c), a comparison between I and Δf can be made. Their relationship is linear; the line shown has a slope of 4.36 Hz/nA. b) Following similar analyses at other biases ($V_{\text{tip}} = -1.5, -1.0, 1.0$ and 1.5 V) the slopes of the fits can be plotted as a function of the bias. I has the opposite sign as V_{tip} . A linear fit is shown as a guide to the eye.

ases ($V_{\text{tip}} = -1.5$ V, -1.0 V, 1.0 V and 1.5 V). Fig. 3(b) shows the slopes of these fits with respect to applied biases. The observation is that not only does this repulsive Δf signal scale linearly with current, but that this $\Delta f/I$ slope itself scales with applied bias voltage.

We then performed measurements with the high-doped sample. At room temperature, this Δf contrast was not observable in the current range of $|I| < 5$ nA. At 4.2 K, however, it was, as shown in Fig. 3(a): In cooling the system, the effective resistance increased and this Δf contrast was again easily observed.

In order to investigate the tip-sample distance, the bias was reduced to zero partway through image acquisition. The result is shown in Fig. 3(b). In this case, the contrast in Δf disappears with the lack of an applied bias voltage. Atomic contrast in Δf should be observable without an applied bias voltage [19]. In order to observe Δf contrast with no applied bias voltage, we needed to advance the tip 340 pm closer to the surface. The remainder of the image, in Fig. 3(c) on, clearly shows the expected contrast in Δf .

One might ask what effect removal of the bias voltage has upon the average tip-sample distance, knowing that there is an electrostatic force between tip and sample that scales as the square of the voltage difference [20]. We have found, in agreement with previous studies [21], that a model of the tip that incorporates a spherical apex with a conic structure to account for long-range electrostatic

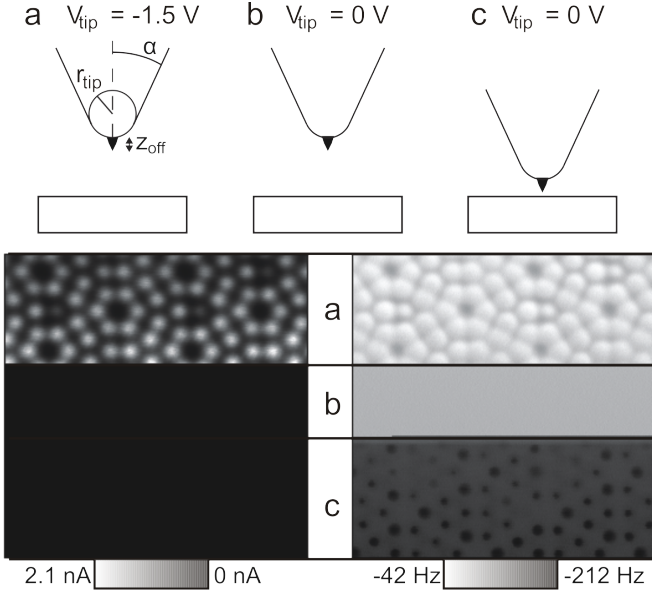


FIG. 3. *Top*: Schematic of the experiment. *Bottom*: Simultaneous I and Δf data acquired at 4.2 K. a) $V_{\text{tip}} = -1.5$ V. b) $V_{\text{tip}} = 0$ V. c) Tip is approached 340 pm closer to the surface. Data were collected at $A = 100$ pm, $f_0 = 16\,777$ Hz and images are $8\text{ nm} \times 8\text{ nm}$.

interactions and a small nano-tip with negligible electrostatic contributions but with which imaging is performed, as shown in Fig. 3(a), is quite accurate when describing long-range electrostatic forces. Typical values to describe our tips are $r_{\text{tip}} = 5$ nm, $\alpha = 70^\circ$, and $z_{\text{off}} = 1$ nm, resulting in an average force, over one oscillation, of 30 nN when $V_{\text{tip}} = 2$ V. Following [18], the effect of removing this bias is that the average tip-sample distance would increase by only 17 pm. Thus, even accounting for the effect of removing the bias voltage, we needed to approach the tip over 300 pm to the surface to observe the Δf contrast in Fig. 3(c). It is therefore not possible that the frequency shift increase (e.g. in Fig. 1 or Fig. 3(a)) was recorded in region I where Pauli repulsion dominates.

We now consider the effect of the sample having a resistance given by R_s , with the tip biased at V_{tip} . The electrostatic interaction between tip and sample causes a force that scales as the square of the voltage difference, $(V_{\text{tip}} - V_{\text{sample}})^2$. We neglect the contact potential difference, V_{cpd} , because it is simply an offset of the applied bias voltage. While local variations in V_{cpd} have been reported on the 7×7 surface with Kelvin probe measurements [22], they would not lead to an increase in Δf over adatoms in both bias polarities. Letting K represent the prefactor which is independent of bias [20]:

$$F^{es} = -K (V_{\text{tip}}^2 - 2V_{\text{tip}} I R_s + I^2 R_s^2) \quad (1)$$

Assuming $V_{\text{sample}} = I R_s \ll V_{\text{tip}}$, the second order term can be discarded. Proceeding with the derivative to k_{ts} ,

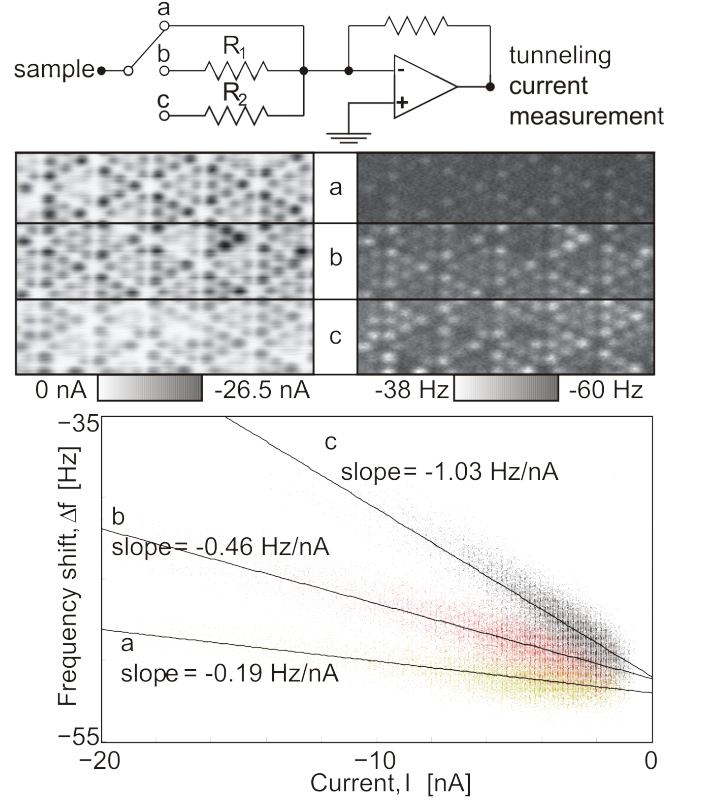


FIG. 4. *Top*: Schematic of the experiment. *Middle*: Simultaneous I and Δf data. *Bottom*: Δf versus I data. a) Data was acquired with no additional resistor between sample and virtual ground. b) $R_1 = 10\text{ M}\Omega$ was inserted between sample and ground. c) $R_2 = 30\text{ M}\Omega$ was inserted. See text for details. Data were acquired with $A = 400$ pm, $f_0 = 19\,390$ Hz and images are $10\text{ nm} \times 7\text{ nm}$.

where $I = I_0 \exp(-\kappa z)$:

$$k_{ts}^{es} \equiv -\frac{dF^{es}}{dz} = \frac{dK}{dz} V_{\text{tip}}^2 - \left(2 \frac{dK}{dz} - 2K\kappa\right) V_{\text{tip}} R_s I \quad (2)$$

Δf is, in the small amplitude approximation, directly proportional to k_{ts} , and if k_{ts}^{es} is dominant, Δf would have a linear response with respect to I and a slope that is linearly proportional to V_{tip} .

To test this theory, we performed an experiment shown schematically in the top third of Fig. 4. A switch was installed between the high-doped sample and the virtual ground. The virtual ground is provided by the operational amplifier used to detect the tunneling current. The switch is used to add known resistances $R_1 = 10\text{ M}\Omega$ and $R_2 = 30\text{ M}\Omega$. Δf should now follow the relation:

$$\Delta f = b + m V_{\text{tip}} (R_s + R) I \quad (3)$$

where R is either 0, R_1 or R_2 , depending on the switch, m is independent of R_s , V_{tip} and I , and b is independent of I . Considering the I -dependent term in Eq. 3, m and R_s are unknown. The data collected at $R = 0$ and $R = R_1$

can be used to determine m and R_s , and then to predict a slope of -0.99 Hz/nA when $R = R_2$. The data and the slopes for the three switch settings are shown in Fig. 4; the observed slope when $R = R_2$ is -1.03 Hz/nA.

This strong agreement with our simple model, incorporating a sample resistance R_s , prompts us to further explain the mechanism of this model. Our fit parameters, for example, indicate that for the low-doped sample $R_s = 164$ M Ω . While this number seems high, the tunneling current is injected in a very small area, and that this in effect creates a large current density that must disperse through a relatively small area. Assuming that the current I is injected in an area of radius 1 Å, and then disperses through the sample radially, we can use classical electrodynamics to determine the order of magnitude of the expected resistance. The current density then scales as $1/(2\pi r^2)$, where r is the distance from the current injection, and is directly proportional to the derivative of the electrochemical potential via the sample resistivity. The voltage between the area in which the tunnel current is being injected and a position in the bulk sufficiently far is thus

$$V_{\text{sample}} = R_s I = \frac{\rho}{2\pi(1\text{ \AA})} I \quad (4)$$

Given this sample has a resistivity $\rho = 6$ to 9 Ω cm, R_s is in the range of 96 to 143 M Ω , which agrees well with the fitted R_s value. In this simple picture, the voltage drop would be highly local, but the charge density and electric field are both most intense near the tip apex, where one would expect the highest contribution to the electrostatic attraction. This picture also has a much higher error when we consider the high-doped sample, and it is likely that an atomic-scale theory of electronic conductance is required to fully explain the observed R_s .

To summarize, we observe a frequency shift increase over adatoms that scales linearly with current. We have characterized this response to current as a function of bias voltage. This frequency shift can be explained by the effect that the tunnel current has on the surface potential, given non-negligible sample resistivity.

As far back as simultaneous FM-AFM and STM have been attempted, contrast inversion has been observed as function of tip state and of applied bias voltage [7–9]. Guggisberg and coworkers suggest that short-range electrostatics might explain the contrast inversion, but do not propose a model for this [10]. Contrast inversion can be explained within our model quite easily: At low biases, the tip images the adatoms as predicted by theory, and shows a negative Δf contrast over adatoms, while at higher biases, the Δf contrast is due primarily to the decrease in capacitive attraction due to the sample resistance and tunnel current, as reported in this Letter.

High spatial resolution demands short-range forces, which implies small tip-sample distances. Given an inter-

est in simultaneous AFM and STM, one must be aware that a moderate tip-sample bias can also produce a tunnel current so large that it would affect the surface potential and measurable Δf contrast. For surfaces such as Cu, with a $\rho \approx 2 \times 10^{-8}$ Ω m, this effect is ignorable [6]; even at $V_{\text{tip}} = 10$ V and $I = 100$ nA, the expected Δf would be < 1 mHz. However this effect must be taken account of when performing combined STM/AFM of any surface with appreciable resistivity, including, of course, semiconductor surfaces.

We thank J. Repp, M. Emmrich and M. Schneiderbauer for discussions and J. Mannhart for support.

-
- [1] G. Binnig, H. Rohrer, C. Gerber, and E. Weibel, *Phys. Rev. Lett.* **50**, 120 (1983).
 - [2] G. Binnig, C.F. Quate, and C. Gerber, *Phys. Rev. Lett.* **56**, 930 (1986).
 - [3] F. Giessibl and G. Binnig, *Ultramicroscopy* **42-44**, 281 (1992).
 - [4] F. J. Giessibl, *Science* **289**, 422 (2006).
 - [5] L. Gross, F. Mohn, N. Moll, P. Liljeroth, and G. Meyer, *Science* **325**, 1110 (2009).
 - [6] M. Ternes, C. González, C.P. Lutz, P. Hapala, F.J. Giessibl, P. Jelínek, and A.J. Heinrich, *Phys. Rev. Lett.* **106**, 016802 (2011).
 - [7] S. Molitor, P. G uthner, and T. Berghaus, *App. Surf. Sci.* **140**, 276 (1999).
 - [8] T. Arai and M. Tomitori, *Jpn. J. Appl. Phys., Part 1*, 3753 (2000).
 - [9] T. Arai and M. Tomitori, *Appl. Surf. Sci.* **157**, 207 (2000).
 - [10] M. Guggisberg, O. Pfeiffer, S. Sch ar, V. Barwich, M. Bammerlin, C. Loppacher, R. Bennewitz, A. Baratoff, and E. Meyer, *App. Phys. A Mat. Sci. & Proc.* **72**, S19 (2001).
 - [11] Y. Sugimoto, Y. Nakajima, D. Sawada, K.-i. Morita, M. Abe, and S. Morita, *Phys. Rev. B* **81**, 245322 (2010).
 - [12] T. Albrecht, P. Grutter, D. Horne, and D. Rugar, *J. Appl. Phys.* **69**, 668 (1990).
 - [13] F. J. Giessibl, *App. Phys. Lett.* **78**, 123 (2001).
 - [14] P. Jelínek, M. Švec, P. Pou, R. Perez, and V. Ch ab, *Phys. Rev. Lett.* **101**, 176101 (2008).
 - [15] N. Moll, L. Gross, F. Mohn, A. Curioni, and G. Meyer, *New J. Phys.* **12**, 125020 (2010).
 - [16] R. P erez, M. C. Payne, I. Stich, and K. Terakura, *Phys. Rev. Lett.* **78**, 678 (1997).
 - [17] R. J. Hamers, R. M. Tromp, and J. E. Demuth, *Phys. Rev. Lett.* **56**, 1972 (1986).
 - [18] S. Hembacher, F. J. Giessibl, and J. Mannhart, *Science* **305**, 380 (2004).
 - [19] F. Giessibl, *Science* **267**, 68 (1995).
 - [20] S. Hudlet, M. Saint Jean, C. Guthmann, and J. Berger, *Eur. Phys. J. B* **2**, 5 (1998).
 - [21] M. Guggisberg, M. Bammerlin, C. Loppacher, O. Pfeiffer, A. Abdurixit, V. Barwich, R. Bennewitz, A. Baratoff, E. Meyer, H.J. Guntherodt, *Phys. Rev. B* **61**, 11151 (2000).
 - [22] S. Sadewasser, P. Jelínek, C.-K. Fang, O. Custance, Y. Yamada, Y. Sugimoto, M. Abe, and S. Morita, *Phys. Rev. Lett.* **103**, 266103 (2009).